# Controlling colloidal processing of $(K, Na)NbO_3$-based materials in aqueous medium

Michel Venet[a,*], Washington Santa-Rosa[a], Jean-Claude M'Peko[b], Harvey Amorín[c], Miguel Algueró[c], Rodrigo Moreno[d]

[a] *Departamento de Física, Universidade Federal de São Carlos, 13565-905, São Carlos, SP, Brazil.*
[b] *Instituto de Física de São Carlos, Universidade de São Paulo, 13560-970, São Carlos, SP, Brazil.*
[c] *Instituto de Ciencia de Materiales de Madrid, CSIC. Cantoblanco, 28049 Madrid, Spain.*
[d] *Instituto de Cerámica y Vidrio (ICV), CSIC. Cantoblanco, 28049 Madrid, Spain*

**Abstract**

$K_{0.5}Na_{0.5}NbO_3$-based materials are serious candidates to replace lead-based piezoceramics since they show excellent electrical and piezoelectric properties. The tape casting technique can be used to obtain highly textured KNN-based ceramics; however, despite industrial and environmental advantages of water-based processing, there are not reports about the control of colloidal processing conditions to obtain optimized $K_{0.5}Na_{0.5}NbO_3$-based slurries in aqueous medium. This paper reports a procedure for controlling colloidal stability and rheological behavior of aqueous $(K_{0.5}Na_{0.5})_{0.97}Li_{0.03}Nb_{0.8}Ta_{0.2}O_3$ suspensions. Zeta potential and cationic solubility measurements as a function of pH showed that pH 8.5 is adequate for concentrated suspensions, while flow curves analysis allowed optimizing processing parameters, such as, powder content, amount of deflocculant and

*Corresponding author
*Email address:* venet74@df.ufscar.br (Michel Venet)

*Preprint submitted to Journal of the European Ceramic Society*

binder, and sonication time. Optimized colloidal suspensions were prepared and used to obtain high quality tapes. Processed ceramics from these stacked tapes show equivalent properties to those processed directly from powders, which demonstrates the effectiveness of the colloidal route reported here.
*Keywords:* Lead-free, KNN, Aqueous tape casting, Colloidal suspensions, Rheological properties

---

## 1. Introduction

Lead-based $Pb_{1-x}Zr_xTiO_3$ (PZT) materials have lead the global market of piezoceramics for many years. Nevertheless, in the last two decades environmental regulations, like EU-Directive 2002/95/EC RoHS, list lead as a hazardous substance and restrict its use in electronic devices, which has considerably increased research demand for lead-free alternatives [1, 2]. Among candidates, $K_{0.5}Na_{0.5}NbO_3$ (KNN)-based materials have aroused great interest since, like PZT's, they crystallize with perovskite structure and present a morphotropic phase boundary, where piezoelectric properties are enhanced [3–5]. Particularly, Ta and Li-doped KNN compositions have shown high Curie temperatures (200-400 $^o$C), high electromechanical coupling factors and piezoelectric coefficients $d_{33}$ values between 200 and 300 pC/N [4, 6–9], which can be considerably increased above 400 pC/N in textured ceramics [4]. These characteristics place KNN-based materials, mainly textured ones, as serious candidates to replace PZT in several applications [10]. KNN based materials have been produced by dry pressing. However, this technique only allows one to prepare monolithic materials but there are some applications in which a laminar structure is required. Laminates with tailored disposition

of layers with controlled composition and thickness cannot be produced by powder pressing and thus, colloidal processing technologies are needed for the preparation of tailored laminated microstructures.

Tape casting is a well-established technique to obtain ceramic tapes that have been used for fabrication of substrates, multilayered ceramic capacitors or composites, solid oxide fuel cells, functionally graded ceramics, and other complexly shaped materials [11–18]. These technologies demand materials with specific properties, that must be reproducible in laboratory and industrial scale. Therefore, knowledge and control of the colloidal stability of the starting suspensions are the key to obtain stable slurries with adequate rheological properties [15, 16]. Solvents, such as hydrocarbons, alcohols or ketones are commonly preferred since uniform green tapes are easily achieved from these solvent types. Aqueous slurries are sensitive to small variations in drying conditions or film thickness, which hinders processing of high-quality tapes when all variables are not well controlled [19–21]. Tape casting has been also useful to process textured or multilayered KNN-based materials; however, in all cases slurries have been prepared from organic solvents without any reported study about control of colloidal processing conditions to optimize slurries [4, 22–26].

Considering the aforementioned points and the distinctive advantages of aqueous fabrication routes, such as incombustibility, low cost and non-toxicity, this work reports the influence of different processing parameters on the aqueous casting of high quality KNN-based tapes and their subsequent use for processing ceramics. Microstructural and property characterization were carried out to demonstrate the effectiveness of the colloidal processing.

## 2. Experimental

$(K_{0.5}Na_{0.5})_{0.97}Li_{0.03}Nb_{0.8}Ta_{0.2}O_3$ (labeled henceforth as LKNNT) powder was synthesized by solid state reaction from precursors $K_2CO_3$ (Aldrich, > 99 % pure), $Na_2CO_3$ (Aldrich, > 99 % pure), $Li_2CO_3$ (Alfa Aesar, > 99.999 % pure), $Nb_2O_5$ (CBMM, > 99.5 % pure) and $Ta_2O_5$ (Across, > 99.99 % pure). Successive calcinations at 750 $^o$C and 800 $^o$C for 5 h were carried out with intermediate ball milling for 24 h [27, 28]. Calcined powder was subjected to high energy milling to reduce particle size in a homemade high energy vibratory mill and the final particle size was verified through a Horiba LA-960 (Horiba, Japan) laser particle size analyzer.

Zeta potential characterizations were performed with a Zetasizer NanoZS equipment (Malvern, UK), based on the laser doppler electrophoresis technique. Suspensions were prepared in deionized water having a solid concentration of 1 g.l$^{-1}$ with $10^{-2}$M KCl as inert electrolyte. On the other hand, concentration levels of dissolved species were measured in suspensions with 1 wt.% of solids content in deionized water, by inductively coupled plasma-optical emission spectrometry (ICP-OES) through a Thermo Jarrell Ash Iris Advantage Spectrometer (Thermo Jarrell Ash, USA). For these measurements, the suspensions were maintained at each prefixed pH for 1 h and subsequently centrifuged to separate the solid from the liquid fraction, which was used for ICP-OES measurements. Suspensions for the characterization of zeta potential and concentration levels of dissolved species were prepared to pH values adjusted between 1 and 10 with HCl or KOH, the natural pH being around 8.5. Polymeric Hypermer KD2 (Croda, UK) and Duramax B-1000 (Rohm & Haas, USA), which are water-soluble, were used as deflocculant and

binder, respectively, and they were added to suspensions as a percent of the powder weight. This binder is an acrylic emulsion in water with 55 % active matter. The solids contents are expressed without considering the dilution promoted by the binder addition. Stirring and dispersion processes were performed using a mechanical stirrer IKA RW20 (IKA, Germany) at typical speeds of 600-800 rpm, and an ultrasound probe UP400S (Dr. Hielscher, Germany) operating under pulsed mode to avoid excessive heating (with a frequency of 50 %). Rheological characterizations were carried out with a rotational rheometer Haake MARS (Thermo-Haake, Germany) at 25 $^o$C by changing shear rate between 0 and 1000 $s^{-1}$ during 3 min, for the up and down ramp, and a stay of 1 min at the maximum rate. The measuring system was a double cone and plate configuration with a cone angle of $2^o$ and a diameter of 60 mm. Suspensions for rheological measurements were prepared to solids loadings of 20 vol.% (i.e. 55 wt.%) in order to optimize the dispersing conditions, including both the deflocculant content and the sonication time. These conditions were extrapolated to more concentrated suspensions (25 vol.% before binder addition and up to 35 vol.% with binder addition). This procedure was selected in order to maximize the solids loading while maintaining the fluidity. However, the addition of binder introduces also a large amount of water and the viscosity decreases significantly. Then it is possible to add more particles after the addition of binder. The real solids loadings of binder containing suspensions are lower due to the dilution effect of the binder (23.7 vol.% and 32.4 vol.% for suspensions with 25 and 35 vol.% solids, respectively).

Tape casting was performed at 30 $mm.s^{-1}$ with a blade height of 200 $\mu$m

onto a Mylar film using suspensions with solids contents ranging from 25 to 35 vol.%, different concentrations of deflocculant (1-3 wt.%) and 10 wt.% of binder. Tapes were dried for 48 h at room temperature without airflow and then, they were cut into squares (1x1 $cm^2$). After that, squares were stacked to form a block, which was uniaxially pressed at 2 MPa. Subsequently, organics were removed at 500 $^o$C for 1 h using heating and cooling rates of 1 $^o$C/min and the green density was determined by the geometrical method. Then, the sample was conventionally sintered at 1110 $^o$C for 2 h in air.

X-ray diffraction (XRD) data were collected at room temperature in the range 20-60$^o$ ($2\theta$), using an AXS D8 Advance diffractometer (Bruker, USA) with CuK$\alpha$ radiation. Ceramic density was also measured by geometric method and relative densification was calculated using the cell parameters, derived from XRD data. A field emission FEI Nova NanoSEM 230 microscope (FEI, Japan) was used for the scanning electron microscopy (SEM) characterization of the powders and polished ceramic surfaces.

Silver electrodes were painted on the ceramic surfaces and then sintered at 600 $^o$C to obtain a parallel plate capacitor for electrical characterizations. Temperature dependence of the dielectric permittivity was dynamically measured, at 1 kHz, with a E4980A precision LCR Meter (Keysight, USA). Hysteresis loop measurements were performed at 0.1 Hz, applying high voltage sine waves, by combination of a HP 3325B function generator (HP, USA), a high voltage amplifier TREK model 10/40 (TREK, Japan) and a homebuilt charge to voltage converter. Finally, ceramic was poled at 120 $^o$C under an electric field of 5 kV.mm$^{-1}$ and the $d_{33}$ piezoelectric charge coefficient was measured with a Berlincourt-type piezometer.

## 3. Results and Discussion

Evaluation of the initial powder characteristics is important in tape casting technique because rheological properties and colloidal stability are sensitive to the particle size distribution as well as their specific surface and shape [15]. Besides, small particle size and narrow size distributions are preferred for a homogeneous particle packing during the sintering process, even though this can make difficult the preparation of concentrated suspensions. Fig. 1 shows the milling time dependence (in a high energy vibratory mill) of the average particle size for the LKNNT powder, and the particle size distribution for the unmilled and milled powder during 6 h. Average particle size was reduced from 1.5 to 0.4 $\mu$m, after a 6 h milling and the particle size distribution was considerably narrowed. This can be also observed in the SEM micrographs of both, unmilled and milled powders, given in Fig. 2a and 2b, respectively. During milling the reduction in size for 6 h (0.4 $\mu$m) is about 73 % of the starting size (1.5 $\mu$m). Further reduction to 0.2 $\mu$m needs another 6 h treatment (with the increased risk of larger contamination) and means a further reduction of less than 15 %. Thus, we selected 6 h milling to prevent excessive contamination and energy consumption. The resulting submicron size is in the typical range of most frequent oxides in technical ceramics, where the measured average particle size is fine enough to prevent fast sedimentation and to allow an easy dispersion. Therefore, the milled powder during 6 h was chosen as the initial LKNNT powder for the following study. The density of the milled powder measured by He picnometry (Multipycnometer, Quantachrome, USA) was 5.0 g.cm$^{-3}$.

Colloidal stability was studied by analyzing the zeta potential as a func-

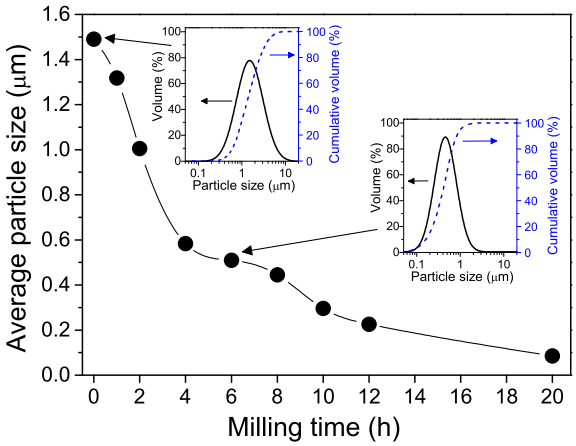


Figure 1: Milling time dependence of the average particle size for the LKNNT powder. Inside, the particle size distribution for unmilled and milled powder during 6 h.

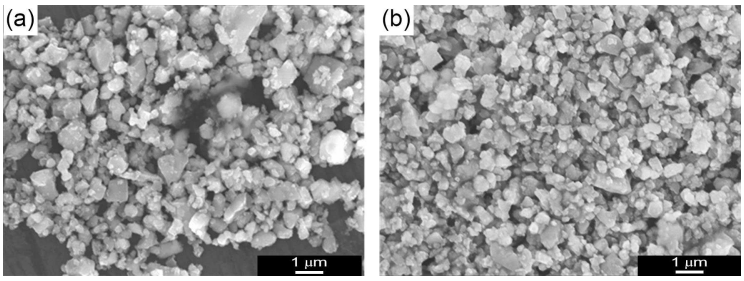


Figure 2: SEM micrographs of LKNNT powders, (a) unmilled and (b) milled during 6 h.

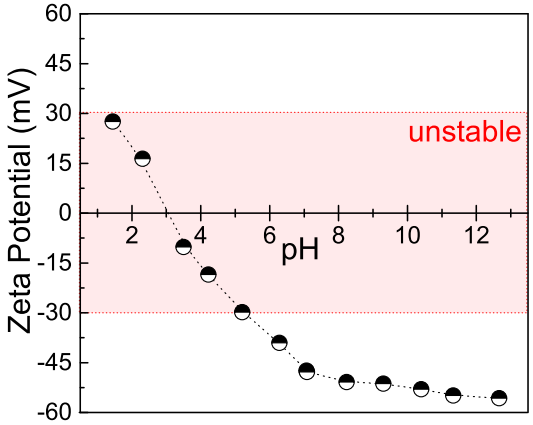


Figure 3: Zeta potential as a function of pH for LKNNT suspensions in aqueous medium.

tion of pH for the LKNNT suspensions in aqueous medium without deflocculant or binder, as illustrated in Fig. 3. Zeta potential shows a high dependence of pH for values lower than pH 8.0 and the isoelectric point occurs around pH 3.0. Stability through Brownian motion requires to prevent particles sticking during collisions; thus, the stable region ($|ZetaPotential| > 30$ mV) was found for pH values above 5.2, where the resultant of the attractive and repulsive forces avoids excessive particle approaching. Natural pH of the LKNNT aqueous suspensions was 8.5, which is inside of the stable region and gives the highest absolute values of zeta potential.

Fig. 4 illustrates the concentration of dissolved cations in distilled water, evaluated as a function of pH. Elements as Na, Li, Nb, and Ta showed solubilities lower than 3 mg.L$^{-1}$, at the natural pH (8.5) of the LKNNT suspensions, which are too low to cause any compositional deviation of the final material. Nevertheless, potassium showed a considerable solubility in the whole pH range, being about 350 mg.L$^{-1}$ for pH 8.5. This can be an issue

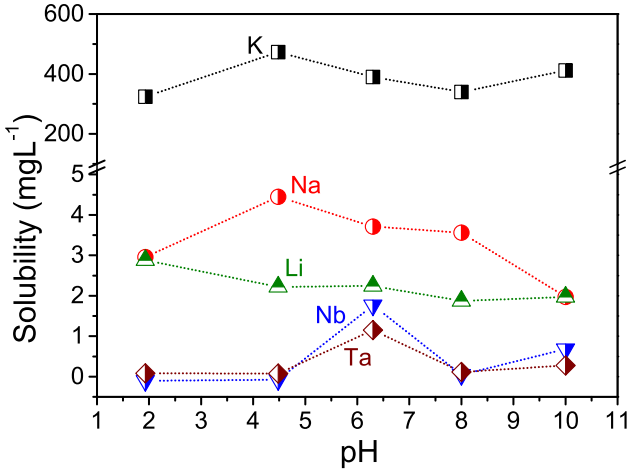


Figure 4: Concentration profiles of dissolved species in distilled water as a function of pH for LKNNT suspensions.

for sustaining stoichiometry and consequently affecting the final electrical properties. However, in tape casting, the whole suspension is used, without discard of any residual medium; in this way, there is a high probability that dissolved potassium reincorporates into the material during sintering process. Electrical characterization of the sintered material will allow to verify if there was, in fact, a drastic compositional deviation or not.

Zeta potential was also evaluated for suspensions with different percentages of deflocculant KD2 (1, 2, and 3 wt.%) at pH 8.5, as shown in Fig. 5. Results show that for this pH value, the zeta potential remains in the stable region without considerable variations for any deflocculant content and without deflocculant, indicating that for these LKNNT suspensions, KD2 acts by steric hindrance.

Once the stability conditions for diluted suspensions were established, LKNNT concentrated suspensions were prepared with a solids loading of 20

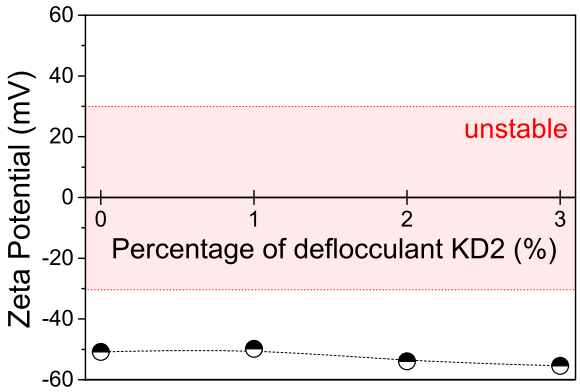


Figure 5: Zeta potential as a function of percentage of deflocculant KD2 at pH 8.5 for LKNNT suspensions in aqueous medium.

vol.% (55 wt.%) at pH 8.5 and the effect of pulsed sonication time and percentage of KD2 deflocculant on the rheology of suspensions was evaluated, as illustrated in Fig. 6. All the samples show thixotropic cycles whose area decrease with increasing sonication time while viscosity tends to increase, probably because the formation of complex structures among particles. Specially, suspensions sonicated for 1 min have large thixotropic cycles with strong time dependence, which is undesirable for tape casting. In this stage lower viscosity is welcome since it indicates a better particle dispersion; thus, sonication during 2 min seems to be a good choice since thixotropy decreases with respect to those sonicated for 1 min, and viscosity remains lower than for 3 min sonication.

On the other hand, samples with 2 wt.% of KD2 deflocculant showed viscosity values lower than those in samples containing 1 or 3 wt.%, for same sonication times. In this way, 2 min of pulsed ultrasound and 2 wt.% of KD2 deflocculant were chosen as acceptable conditions to carry on with

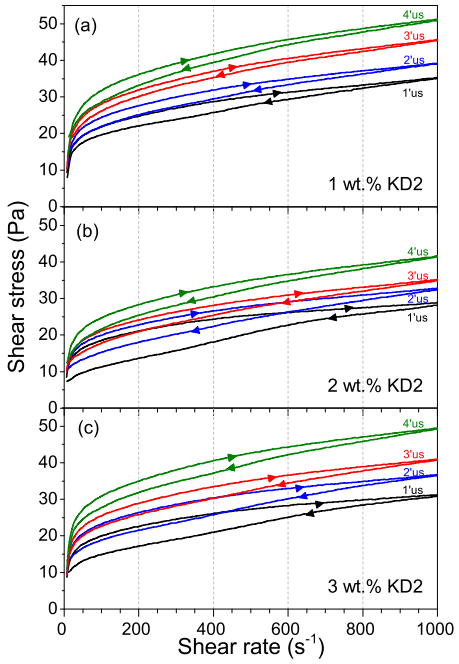


Figure 6: Flow curves for LKNNT concentrated suspensions without binder addition, with a solids loading of 20 vol.% at pH 8.5 and with (a) 1, (b) 2, and (c) 3 wt.% of KD2 deflocculant, subjected to different sonication times (x'us = x min of pulsed ultrasound).

the rheology study. Table 1 summarizes the values of the thixotropic area and viscosity at the shear rate of 150 $s^{-1}$ ($\eta(150\ s^{-1})$) for all these LKNNT suspensions. This shear rate was calculated as the ratio between used cast velocity and blade height.

Tapes with high green density and low drying shrinkage require slurries with high solids content [29, 30]. Therefore, powder content was gradually increased in suspensions with 2 wt.% of KD2 up to solids loading higher than 25 vol.%. The flow curve of the slurry with 25 vol.% of ceramic powder without binder, which is represented as circles in Fig. 7, shows a significant increase of the viscosity with respect to that containing 20 vol.% (see Fig.

Table 1: Thixotropic area (TA) and viscosity at the shear rate of 150 $s^{-1}$ ($\eta$(150 $s^{-1}$)), for LKNNT concentrated suspensions without binder addition, with a solids loading of 20 vol.% at pH 8.5 and with 1, 2, and 3 wt.% of KD2 deflocculant, subjected to sonication for different times (ST).

| **KD2 (wt.%)** | **ST (min)** | **TA ($Pa.s^{-1}$)** | **$\eta$(150 $s^{-1}$) (mPa.s)** |
|---|---|---|---|
| 1 | 1 | 1551 | 152.0 |
| | 2 | 1288 | 174.3 |
| | 3 | 785 | 196.9 |
| | 4 | 1491 | 228.3 |
| 2 | 1 | 4198 | 129.9 |
| | 2 | 2807 | 141.1 |
| | 3 | 1719 | 147.5 |
| | 4 | 1632 | 174.7 |
| 3 | 1 | 3149 | 143.1 |
| | 2 | 2749 | 163.1 |
| | 3 | 1685 | 180.5 |
| | 4 | 1869 | 216.6 |

6b). After the binder addition in the proportion of 10 wt.% with respect to the powder weight, viscosity considerably falls, as illustrated by its flow curve (triangles) in Fig. 7. This is expected due to the slurry dilution by the addition of the water (45 %) contained in the binder emulsion. Aspect of the dry tape, cast from this slurry, can be found in the picture at right bottom corner of Fig. 7. Tape exhibits defects along edges and shrinkage at the end because of the excessive decreasing of the slurry viscosity. This indicates it is necessary to increase the solids loading in order to recover the initial viscosity. Flow curve represented as squares in Fig. 7 shows the rheological behavior of a slurry with a 10 wt.% of binder, whose solids content had been increased up to 35 vol.%. The thixotropy increases to 12000 $Pa.s^{-1}$ for this solids loading. The new dry tape can be seen in the picture at the right top

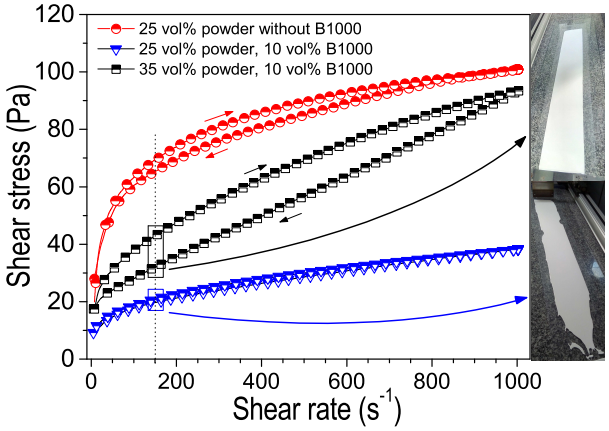


Figure 7: Flow curves for LKNNT slurries with different solid volumes without and with binder addition. On the right-side images of the tapes cast from the slips with binder are shown.

corner. This cast tape was easily peeled out showing high flexibility without any macroscopic defect and adequate green density (53 % th); therefore, it was used to obtain ceramic specimens for subsequent characterizations.

Sintered ceramic specimens prepared by stacking 25 tape pieces were characterized by XRD to control the absence of possible secondary phases or modification of the crystalline structure. XRD pattern in Fig. 8a shows characteristic mixture of the orthorhombic (Bmm2) and tetragonal (P4mm) phases, which is expected for the studied composition, since doping in KNN brings the polymorphic phase transition (orthorhombic to tetragonal) down to room temperature, where both phases can coexist [31]. No additional secondary phases were identified. On the other hand, the relative density was 94 % of theoretical assuming no secondary phases. The microstructure of the transversal section of a characteristic ceramic sample, shown in Fig. 8b, does not indicate any anomaly that could be associated with the intersection

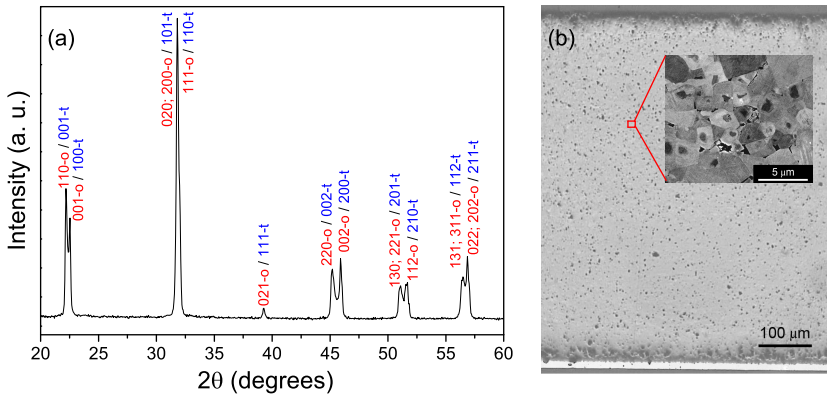


Figure 8: (a) XRD pattern and (b) micrograph of the transversal section with a zoom inside image for a LKNNT ceramic obtained from the stacked tapes. XRD peaks were indexed using cards 04017-0216 (orthorhombic) and 04017-0217 (tetragonal) from PCPDF database.

between stacked tapes, which would have a unitary thickness around 40 $\mu$m after sintering. This demonstrates that an intimate contact among layers was achieved. The zoom in Fig. 8b reveals grains with typical core-shell structure. This is usually observed in Li and Ta-doped KNN materials prepared from powders, obtained by the solid state via [18, 32, 33] and it is related to compositional inhomogeneities, where Nb- and K-rich cores are surrounded by Ta-rich shells [33].

Fig. 9a shows the real and imaginary part of the permittivity, measured at 1 kHz, as a function of temperature for the LKNNT ceramic obtained from the stacked tapes. A characteristic peak, related with the ferroelectric-paraelectric phase transition, occurs around Curie temperature of 345 $^o$C, in both, real and imaginary parts of permittivity. Curie temperature is extremely sensitive to compositional modifications in KNN-based materials [6, 34]. In fact, an additional slight anomaly takes place at $\backsim$420 $^o$C

(small shoulder), which is the temperature of the paraelectric-ferroelectric phase transition of $K_{0.5}Na_{0.5}NbO_3$ [3]. This is a result of the core-shell microstructure where compositional deviations occur, with KNN cores surrounded by LKNNT shells. Inset in Fig. 9a shows the real permittivity, at 1 kHz, for $(K_{0.5}Na_{0.5})_{1-x}Li_xNb_{1-y}Ta_yO_3$ ceramics with different compositions, which where conventionally sintered directly from powders without colloidal processing. Large variations of the Curie temperature with small compositional differences, illustrate the high sensibility of Curie temperature to compositional modifications in these materials. Nevertheless, the LKNNT ceramic obtained from the stacked tapes, whose composition is $(K_{0.5}Na_{0.5})_{0.97}Li_{0.03}Nb_{0.8}Ta_{0.2}O_3$ has the same Curie temperature that the ceramic with equal composition, which was conventionally sintered directly from powders without colloidal processing (dry powder processing), such as represented by dotted lines in Fig. 9a and in the inset. This is a convincing indication that potassium solubility at the working pH does not affect the final composition of the targeted material and the dissolved cations reincorporate into the material during the sintering process. Fig. 9b shows the hysteresis loop (polarization vs electric field) for the LKNNT ceramic obtained from the stacked tapes. Coercive field is in accordance with previously published values [8]; however, remnant polarization ($\backsim$11 $\mu$C.cm$^{-2}$) and piezoelectric coefficient $d_{33}$, whose value was 185 pC/N, were somehow smaller than expected for this composition [6, 8], which is a consequence of the core-shell grained microstructure as discussed in previous works [18, 32].

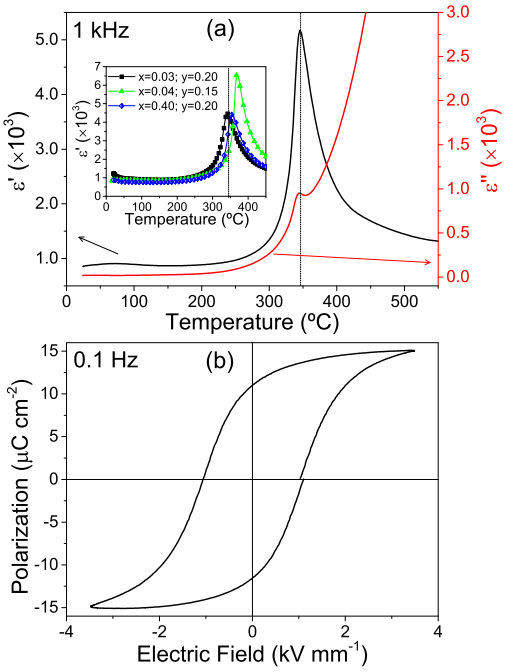


Figure 9: (a) Real and imaginary part of the permittivity, at 1 kHz, as a function of temperature and (b) hysteresis loop (polarization vs electric field) for the LKNNT ceramic obtained from the stacked tapes. Inset in (a) shows the real permittivity, at 1 kHz, for $(K_{0.5}Na_{0.5})_{1-x}Li_xNb_{1-y}Ta_yO_3$ ceramics with different compositions, which where conventionally sintered directly from powders by dry powder processing.

## 4. Conclusions

The successful colloidal processing of KNN-based materials in aqueous medium is demonstrated in this work. Powder with a nominal composition of $(K_{0.5}Na_{0.5})_{0.97}Li_{0.03}Nb_{0.8}Ta_{0.2}O_3$ was obtained by solid state reaction and subsequently milled during 6 h to achieve submicron average particle size (0.4 $\mu$m) and narrow size distribution. Colloidal stability analysis showed that the natural pH of the LKNNT aqueous suspensions (8.5) is inside the stability region and therefore, this was used for concentrated suspensions. Slurries containing 2 wt.% of KD2 deflocculant, 10 wt.% of binder (Duramax B1000), and a final solids loading of 35 vol.%, subjected to pulsed ultrasounds during 2 min, result in high quality flexible tapes without any macroscopic defect and an adequate green relative density of 53 % th. Structural, microstructural and electrical characterization of ceramics processed from these stacked tapes showed equivalent properties to those obtained in conventionally sintered ceramics from powders, but by dry powder processing. Specially, dielectric characterization demonstrated that the potassium cation solubility in water is not an issue in this case, because it apparently reincorporates into the material during the sintering process.

## Acknowledgements

Research co-funded by the Coordenação de Aperfeiçoamento de Pessoal de Nível Superior - Brasil (CAPES) - Finance Code 001 (process 88881.030500/2013-01), São Paulo Research Foundation FAPESP (grants #2013/00134-7 and #2017/17872-1), and Spanish MINECO (projects MAT2014-58816-R, MAT2015-67586-CR-2-R, and MAT2017-88788-R).

## References


[1] Rödel J, Jo W, Seifert KTP, Anton EM, Granzow T, Damjanovic D. Perspective on the development of lead-free piezoceramics. J Am Ceram Soc 2009;92(6):1153–1177. doi:10.1111/j.1551-2916.2009.03061.x.

[2] Maurya D, Peddigari M, Kang MG, Geng LD, Sharpes N, Annapureddy V, et al. Lead-free piezoelectric materials and composites for high power density energy harvesting. J Mater Res 2018;33(16):2235–2263. doi:10.1557/jmr.2018.172.

[3] Jaffe B, Cook WR, Jaffe H. Piezoelectric Ceramics. Academic Press; 1971. ISBN 9780323155687.

[4] Saito Y, Takao H, Tani T, Nonoyama T, Takatori K, Homma T, et al. Lead-free piezoceramics. Nature 2004;432(7013):84–87. doi:10.1038/nature03028.

[5] Mazuera AM, Silva PS, Rodrigues AD, Pizani PS, Romaguera-Barcelay Y, Venet M, et al. Origin of discrepancy between electrical and mechanical anomalies in lead-free $(K, Na)NbO_3$-based ceramics. Phys Rev B 2016;94(18). doi:10.1103/physrevb.94.184101.

[6] Saito Y, Takao H. High performance lead-free piezoelectric ceramics in the $(K, Na)NbO_3$-$LiTaO_3$ solid solution system. Ferroelectrics 2006;338(1):17–32. doi:10.1080/00150190600732512.

[7] Fu J, Santa-Rosa W, M'Peko JC, Algueró M, Venet M. Magnetoelectric coupling in lead-free piezoelectric $Li_x(K_{0.5}Na_{0.5})_{1-x}Nb_{1-y}Ta_yO_3$

and magnetostrictive $CoFe_2O_4$ laminated composites. Phys Lett A 2016;380(20):1788–1792. doi:10.1016/j.physleta.2016.03.024.

[8] Chang Y, pei Yang Z, Ma D, Liu Z, Wang Z. Phase transitional behavior, microstructure, and electrical properties in Ta-modified $[(K_{0.458}Na_{0.542})_{0.96}Li_{0.04}]NbO_3$ lead-free piezoelectric ceramics. J Appl Phys 2008;104(2):024109. doi:10.1063/1.2957591.

[9] Guo Y, ichi Kakimoto K, Ohsato H. $(Na_{0.5}K_{0.5})NbO_3$-$LiTaO_3$ lead-free piezoelectric ceramics. Mater Lett 2005;59(2-3):241–244. doi:10.1016/j.matlet.2004.07.057.

[10] Rödel J, Webber KG, Dittmer R, Jo W, Kimura M, Damjanovic D. Transferring lead-free piezoelectric ceramics into application. J Eur Ceram Soc 2015;35(6):1659–1681. doi:10.1016/j.jeurceramsoc.2014.12.013.

[11] Schileo G, Pascual-Gonzalez C, Algueró M, Reaney IM, Postolache P, Mitoseriu L, et al. 2018;38(4):1473–1478. doi:10.1016/j.jeurceramsoc.2017.10.055.

[12] Schwartz B. Review of multilayer ceramics for microelectronic packaging. J Phys Chem Solids 1984;45(10):1051–1068. doi:10.1016/0022-3697(84)90048-9.

[13] Will J. Fabrication of thin electrolytes for second-generation solid oxide fuel cells. Solid State Ionics 2000;131(1-2):79–96. doi:10.1016/s0167-2738(00)00624-x.

[14] Bever M, Duwez P. Gradients in composite materials. Mater Sci Eng 1972;10:1–8. doi:10.1016/0025-5416(72)90059-6.

[15] Jabbari M, Bulatova R, Tok A, Bahl C, Mitsoulis E, Hattel J. Ceramic tape casting: A review of current methods and trends with emphasis on rheological behaviour and flow analysis. Mater Sci Eng, B 2016;212:39–61. doi:10.1016/j.mseb.2016.07.011.

[16] Moreno R. Colloidal processing of ceramics and composites. Adv Appl Ceram 2012;111(5-6):246–253. doi:10.1179/1743676111y.0000000075.

[17] Amorín H, Ricote J, San-Felipe I, Salazar N, del Campo R, Romaguera-Barcelay Y, et al. Multilayer ceramic magnetoelectric composites with tailored interfaces for enhanced response. ACS Appl Mater Interfaces 2017;9(44):39094–39104. doi:10.1021/acsami.7b14775.

[18] Santa-Rosa W, Venet M, M'Peko JC, Moreno R, Amorín H, Algueró M. Environmentally-friendly magnetoelectric ceramic multilayer composites by water-based tape casting. J Eur Ceram Soc 2019;39(4):1065–1072. doi:10.1016/j.jeurceramsoc.2018.10.009.

[19] Hotza D, Greil P. Review: aqueous tape casting of ceramic powders. Mater Sci Eng, A 1995;202(1-2):206–217. doi:10.1016/0921-5093(95)09785-6.

[20] Gutiérrez CA, Moreno R. Influence of slip preparation and casting conditions on aqueous tape casting of $Al_2O_3$. Mater Res Bull 2001;36(11):2059–2072. doi:10.1016/s0025-5408(01)00683-3.

[21] Luo XJ, Zhang BL, Li WL, Zhuang HR. Comparison of aqueous and non-aqueous tape casting of aluminum nitride substrates. J Am Ceram Soc 2005;88(2):497–499. doi:10.1111/j.1551-2916.2005.00090.x.

[22] Lin Y, Qiu Y, Zhang J, Yang H, Wang T, Yan F. Transverse and longitudinal magnetoelectric effect in multilayer $Li_{0.058}(Na_{0.535}K_{0.48})_{0.942}NbO_3/Co_{0.6}Zn_{0.4}Fe_{1.7}Mn_{0.3O4}$ bulk composites. Appl Phys Lett 2018;112(7):072901. doi:10.1063/1.5008604.

[23] Liu B, Li P, Zhang Y, Shen B, Zhai J. Enhanced piezoelectricity in $(K, Na)NbO_3$-based ceramics by optimizing composition and texture process. J Alloys Compd 2017;695:2207–2214. doi:10.1016/j.jallcom.2016.11.069.

[24] Wang W, Yuan X, Ma C, Tang F, Wang F, Cao Y. Investigation on the phase transition behavior and electrical properties of textured $Li_x(K_{0.48}Na_{0.52})_{1-x}NbO_3$ piezoelectric ceramics. Ceram Int 2015;41(7):8377–8381. doi:10.1016/j.ceramint.2015.03.028.

[25] Zhu B, Zhang Z, Ma T, Yang X, Li Y, Shung KK, et al. (100)-textured KNN-based thick film with enhanced piezoelectric property for intravascular ultrasound imaging. Appl Phys Lett 2015;106(17):173504. doi:10.1063/1.4919387.

[26] Hussain A, Kim JS, Song TK, Kim MH, Kim WJ, Kim SS. Fabrication of textured KNNT ceramics by reactive template grain growth using NN templates. Curr Appl Phys 2013;13(6):1055–1059. doi:10.1016/j.cap.2013.02.013.

[27] Gao R, Chu X, Huan Y, Wang X, Li L. $(K, Na)NbO_3$ based piezoceramics prepared by a two-step calcining and ball milling route. Mater Lett 2014;123:242–245. doi:10.1016/j.matlet.2014.03.027.

[28] Hollenstein E, Davis M, Damjanovic D, Setter N. Piezoelectric properties of Li- and Ta-modified $(K_{0.5}Na_{0.5})NbO_3$ ceramics. Appl Phys Lett 2005;87(18):182905. doi:10.1063/1.2123387.

[29] Greenwood R, Roncari E, Galassi C. Preparation of concentrated aqueous alumina suspensions for tape casting. J Eur Ceram Soc 1997;17(12):1393–1401. doi:10.1016/s0955-2219(97)00034-4.

[30] Rincón A, Chinelatto AS, Moreno R. Tape casting of alumina/zirconia suspensions containing graphene oxide. J Eur Ceram Soc 2014;34(7):1819–1827. doi:10.1016/j.jeurceramsoc.2013.12.027.

[31] Li HT, Zhang BP, Cui M, Yang WG, Ma N, Li JF. Microstructure, crystalline phase, and electrical properties of ZnO-added $Li_{0.06}(Na_{0.535}K_{0.48})_{0.94}NbO_3$ ceramics. Curr Appl Phys 2011;11(3):S184–S188. doi:10.1016/j.cap.2010.12.026.

[32] Santa-Rosa W, Venet M, M'Peko JC, Amorín H, Algueró M. Processing issues and their influence in the magnetoelectric performance of $(K, Na)NbO_3/CoFe_2O_4$-based layered composites. J Alloys Comp 2018;744:691–700. doi:10.1016/j.jallcom.2018.02.083.

[33] Wang Y, Damjanovic D, Klein N, Hollenstein E, Setter N. Compositional inhomogeneity in Li- and Ta-modified $(K, Na)NbO_3$ ceramics. J Am Ceram Soc 2007;90(11):3485–3489. doi:10.1111/j.1551-2916.2007.01962.x.

[34] Zhou JJ, Li JF, Wang K, Zhang XW. Phase structure and electrical properties of (Li,Ta)-doped $(K, Na)NbO_3$ lead-free piezoceramics

in the vicinity of Na/K = 50/50. J Mater Sci 2011;46(15):5111–5116. doi:10.1007/s10853-011-5442-7.